Directional Bend Sensor Based on Re-Grown Tilted Fiber Bragg Grating

Li-Yang Shao, *Member, OSA*, Lingyun Xiong, Chengkun Chen, Albane Laronche, and Jacques Albert, *Member, IEEE, OSA*

***Abstract*—A novel fiber optic bend sensor is implemented by using a re-grown tilted fiber Bragg grating (TFBG) written in a small core single mode fiber with UV overexposure. The spectrum of the re-grown TFBG contrasts with that of normal TFBG by exhibiting large differences in the amplitude between neighboring symmetric (LP_{0m}) and asymmetric (LP_{1m}) cladding mode resonances, moreover each asymmetric cladding mode resonance splits into two peaks (corresponding to two orthogonal polarization states). The differential response of the three individual resonances of such group provides quantitative information about the magnitude and directions of bends in the TFBG. Numerical simulations indicate that the changes in the cladding-mode profiles in a bent fiber are responsible for this behavior through their impact on coupling coefficients. A bend sensitivity of 0.4 dB. m (for the 18th order group of cladding modes) is experimentally demonstrated within a range of 0–10.6 m^{-1}.**

***Index Terms*—Bend sensor, birefringence, cladding mode, optical fiber sensors, tilted fiber Bragg grating.**

I. Introduction

FIBER grating sensors have been successfully demonstrated for the detection of physical parameters, such as strain, pressure or bending [1]–[3]. However, one of the practical challenges encountered in real-world applications such as structural health monitoring is the determination of the direction of the applied force or of the bending plane. For example, in ship hull shape sensing applications, it is necessary to determine both the amplitude and orientation of applied bend at the same time (so-called directional or vector sensing) [4]–[8]. Long period gratings (LPGs) have been with some success for these purposes because bending causes shifts in the resonance wavelength or a separation of the resonances when mode splitting occurs, and these changes can be vectorial in nature because of the relative orientation of the bend plane with that of the field profiles of the cladding modes involved [4]–[6].

Manuscript received June 07, 2010; revised July 28, 2010; accepted July 28, 2010. Date of publication August 09, 2010; date of current version August 30, 2010. This work is supported in part by the Natural Sciences and Engineering Research Council of Canada, in part by the Canada Foundation for Innovation, in part by the Canada Research Chairs program, and in part by LxDATA.

L.-Y. Shao is with the Department of Electronics, Carleton University, Ottawa, ON K1S 5B6, Canada, and also with the Institute of Optoelectronic Technology, China Jiliang University, Hangzhou 310018, China (e-mail: liyangshao@gmail.com).

L.Y. Xiong, A. Laronche, and J. Albert are with the Department of Electronics, Carleton University, Ottawa, ON K1S 5B6, Canada.

C.K. Chen is with the School of Information Technology and Engineering, University of Ottawa, Ottawa ON K1N 6N5, Canada.

Color versions of one or more of the figures in this paper are available online at http://ieeexplore.ieee.org.

Digital Object Identifier 10.1109/JLT.2010.2064158

The issue with LPG sensors is two-fold: the resonances are very broad and separated by large wavelength distances (meaning that only a few cladding mode resonances can be observed in a measurement window); and they are also very sensitive to other parameters, including temperature, axial strain and external refractive index. As a result, it is difficult to construct a LPG sensor that will specifically measure bending magnitude and direction over a large range of values without contamination of the data by other effects. Fiber Bragg gratings (FBG) do not suffer from these problems but they are naturally insensitive to bending since the core lies on the neutral stress axis of the bent fiber. Therefore, special schemes have been needed to use FBGs for bend sensing. Flockhart *et al.* have reported a two axis curvature measurement by fabricating FBGs in three separate cores of a multicore fiber [7]. Alternatively, another multi-dimensional bend sensor has been demonstrated by monitoring the amplitude variation and wavelength shift of Bragg resonance with one surface-relief FBG in a D-shaped fiber [8]. However, the use of special fibers in these cases introduces additional complexity in systems and can present splicing problems. In general, the strategy for achieving directional bend sensitivity in both LPG and FBG based solutions is to employ fibers with asymmetrical core or cladding geometries, or introduce an asymmetrical index perturbation in the cross section of fiber by use of CO_2 or femtosecond lasers.

Tilted fiber Bragg gratings (TFBG) present an attractive compromise between the inherent advantages and constraints of FBG and LPG sensors: they can be used to excite a large number of cladding modes in a much narrower spectral bandwidth than LPGs and they have thermal and strain cross sensitivities as low as those of FBGs. For these reasons, TFBGs have been investigated intensively for sensing applications [9]–[16]. In particular for bending, Baek *et al.* have reported a macro-bending sensor by monitoring the shift of a group of low order cladding mode resonances (this group is usually referred to as the "ghost" mode) in TFBGs [9]: the key here is that the tilt plane of the grating breaks the cylindrical symmetry of the fiber and defines a pair of orthogonal directions along which the response of the grating upon bending will be different. This is what makes it possible to determine both of bending amplitude and direction simultaneously, as long as the spectral changes can be quantitatively correlated with these parameters. Unfortunately, the "ghost" mode resonance of TFBG is not ideal because it consists of a superposition of several low-order cladding modes that each reacts differently to bending magnitude and direction: the resulting spectral changes are extremely complex and it becomes difficult to extract meaningful data [10]. Finally, we recently proposed and demonstrated a vector

inclinometer made up of a non-adiabatic abrupt taper cascaded with a TFBG [11]. In that device, the direction and magnitude of a bend can be determined by the relative power levels of the core mode and a group of higher order cladding modes re-coupled through the bent taper. While this last device works well, it requires very careful packaging to make sure the taper does not break.

The purpose of the present paper is to propose and demonstrate an even simpler configuration that does not require an additional core-cladding coupling element in addition to the TFBG. This configuration stems from the understanding that the modal strength spectroscopy (relative amplitudes of the cladding mode resonances in a TFBG spectrum) depends strongly on the fiber characteristics [12]. For small radius and high refractive index core fibers, we have found that TFBG transmission spectrum of a type IA-like re-grown grating (the coupling strength of TFBG decreases to zero then re-grown with continuous UV-exposure just like type IA FBG, but the Bragg wavelength only has a red shift of several hundreds of picometers while that of type IA FBG shifts tens of nanometers to longer wavelength) [13], includes pairs of resonances that react strongly and in opposite directions when the fiber is bent, and further that the spectral changes observed depend relatively simply on the orientation of the bend. Numerical simulations suggest that this phenomenon is partially due to changes in the cladding-mode profiles of the bent fiber, changes that impact the coupling of those modes to the incident core mode. Experimental results show that the bending magnitude and direction can be determined by monitoring a well chosen set of neighboring symmetrical and asymmetrical modes of the same mode order.

II. Fabrication of TFBGs

Corning Flexcore fiber with a core radius of 2.625 μm is used for this work. For comparison, TFBGs fabricated in standard telecommunications fiber (Corning SMF-28) will also be shown. All the fibers were hydrogenated in a hydrogen chamber for 12 days at 2500 psi and room temperature (25°C) to improve their photosensitivity. All gratings considered here are 1-cm-long with a tilt angle of 4° (internal tilt angle) and they were written in hydrogen-loaded fibers by using a 193 nm pulsed ArF excimer laser and the phase mask technique. The repetition rate and energy density of UV laser pulse are 100 Hz and 80 mJ/cm^2, respectively. The spectra of TFBGs are recorded with an unpolarized broadband source (BBS) and an optical spectrum analyzer (OSA) with a resolution of 0.01 nm. Fig. 1(a) shows the measured transmission spectrum of a TFBG in Corning Flexcore fiber in the Type I regime (normal grating growth in increasing fluence); in this case the maximum reflectivity of the core mode reached 45 dB after only 3 seconds of irradiation. A similar grating was written up to a maximum coupling strength (over -50 dB in transmission at the Bragg resonance, we cannot measure the exact transmission because of the limitation of OSA's dynamic range), obtained after 60 seconds of irradiation, and then the irradiation was continued to saturate the grating and re-grow it (corresponding to the Type IA regime) until the core mode reflectivity reached 99%. To distinguish from Type IA and regenerated grating by temperature, it is named as re-grown TFBG (R-TFBG). The resulting spectrum after a total irradiation time of 150 seconds is shown in Fig. 1(b). Finally, Fig. 1(c) illustrates a similar Type I 4° TFBG in SMF-28 fiber. It is clear that the envelope of the cladding mode spectra are quite different for the three cases, reflecting changes in the coupling coefficients between the core mode and the various cladding modes. It is worth noting that the cladding modes of all three cases should be very similar as they all correspond to a 125 μm diameter pure silica rod in air. The most notable difference between the spectra of Fig. 1 is the absence of the "ghost" mode resonance in the Flexcore fiber and, to a lesser extent, a more uniform (flatter) envelope of cladding mode resonances. The ghost mode resonance is well known for TFBGs in standard SMF fibers and corresponds to a group of overlapping low order cladding modes that builds up to a very strong resonance immediately adjacent to the core mode reflection resonance. Of greater interest here, the insets of Fig. 1 show for each grating a set of neighboring $\mathrm{LP}_{0\mathrm{m}}$ and $\mathrm{LP}_{1\mathrm{m}}$ cladding mode resonances located at the wavelength from 1542 nm to 1543 nm. We can see from the insets of Fig. 1(a) and Fig. 1(c) (Type I TFBGs in two kinds of fibers) that $\mathrm{LP}_{0\mathrm{m}}$ and $\mathrm{LP}_{1\mathrm{m}}$ mode resonances have comparable coupling strength. But there is an obvious difference between two groups of modes and the $\mathrm{LP}_{1\mathrm{m}}$ mode split into two in R-TFBG written in the Flexcore fiber, which may related to coupling to a pair of x- and y-polarized asymmetric $\mathrm{LP}_{1\mathrm{m}}$. The R-TFBG is of most interests and employed for the latter bending experiments.

III. Modes of a Bent Fiber

In [9], Baek has claimed the directional bending responses of a TFBG is caused by the change of effective tilt angle in a bent TFBG. This explanation is very straightforward but maybe too simple and not complete. In fact, the diameter of fiber cladding (125 μm) is quite small compared to the radius (10 cm) of a moderate bend (curvature equals to 10 m^{-1}). So the effect of tilt angle changes of TFBG should be tiny. We demonstrate that instead, the coupling strength of cladding mode resonances in TFBG is partially induced by the changes in the symmetry of the modes themselves. Marcuse showed that the modes of bent fibers tend to shift to the outer portion as they propagate around a bend [14]. Thus, the effective indexes of the cladding modes and of core mode also change accordingly [15].

Fig. 2(a) is the schematic diagram of geometry of a bent fiber. The bending on a straight fiber induces a longitudinal strain ε oriented parallel to the optical axis, where $\varepsilon = Cx$ (C is curvature of the bend and equal to the inverse of the bending radius R). Taking the photoelastic effect, this strain introduces an refractive index change Δn in the fiber cross section, where $\Delta n = -(n^3/2)[(1-\nu)p_{12} - \nu p_{11}]Cx$, ν s the Poisson ratio, p_{11} and p_{12} are photoelastic constants, and n is the refractive index [15]. Fig. 2(b) shows the relation between the position at x axis and longitudinal strain induced refractive index change. For a silica fiber at the wavelength of C-band, the slope rate of the linear curve is around $-0.31C$. That means a modified refractive index profile across the fiber cross section with a decrease

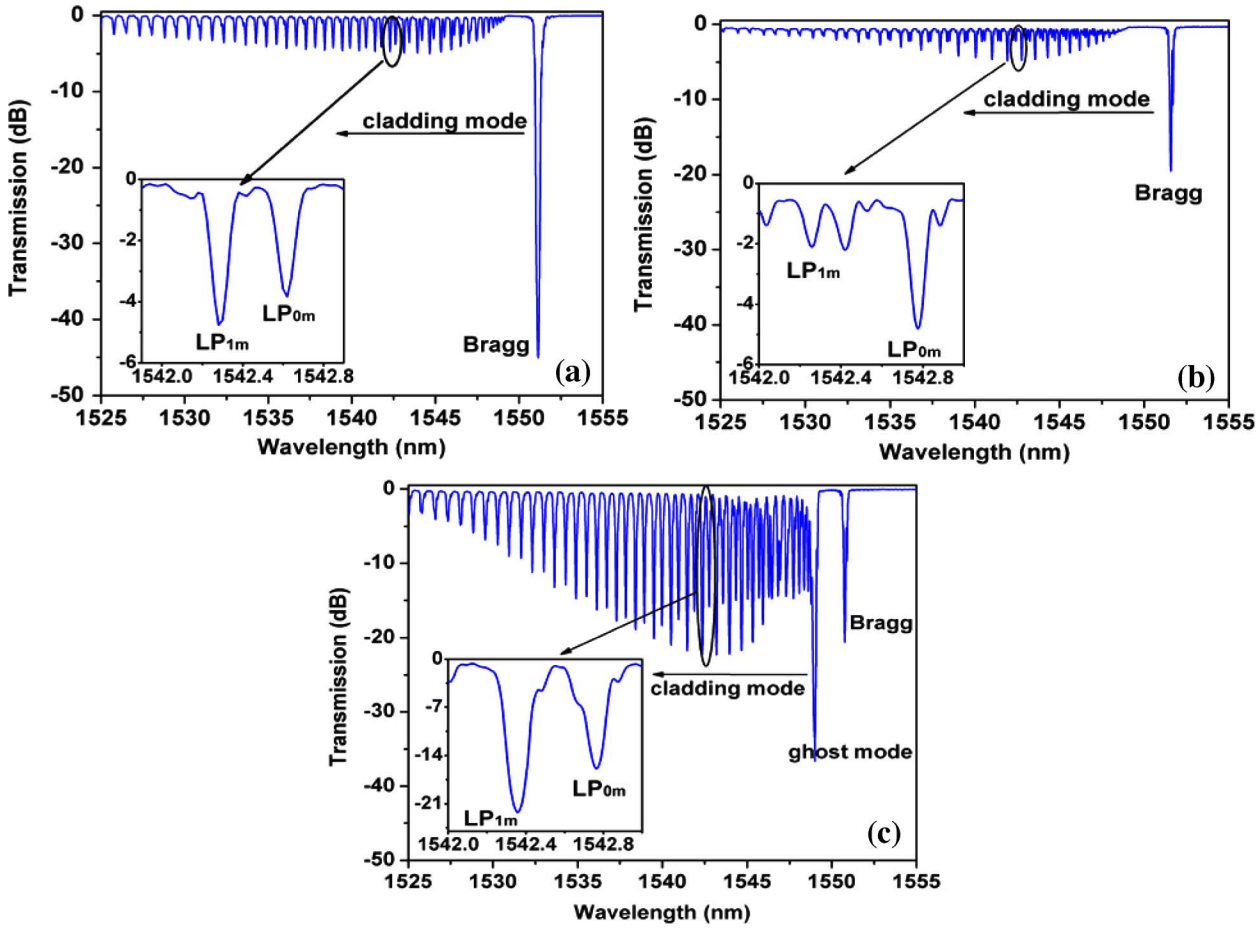

Fig. 1. Spectra of (a) Type I TFBG (b) R-TFBG with UV overexposure in Corning Flexcore fiber (c) Type I TFBG in SMF-28 fiber. The insets of (a) (b) and (c) show the enlarged spectrum of two neighboring $\mathrm{LP}_{0\mathrm{m}}$ and $\mathrm{LP}_{1\mathrm{m}}$ cladding mode resonances around the wavelength from 1542 nm to 1543 nm, respectively.

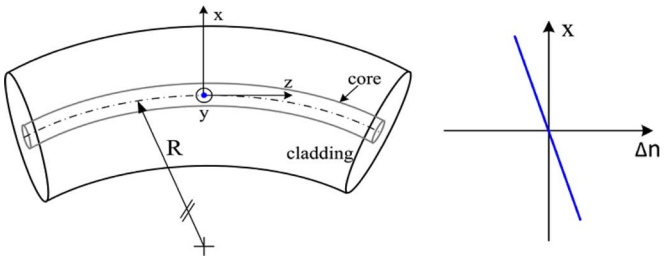

Fig. 2. (a) Geometry of bent fiber; (b) longitudinal strain induced refractive index change along x axis in the bent fiber.

for the outer half stretched portion of fiber and an increase for the inner half compressed portion.

The modes of a bent fiber can be determined through an equivalent straight waveguide (ESW) in terms of a three-layer cylindrical structure of fiber core, cladding, and surrounding medium Here, we have used a commercial available software (Mode Solutions 4.0 from Lumerical Solutions, Inc.) to investigate the interaction between core and cladding modes in a bent fiber [16]. The parameters for Corning Flexcore fiber are as follows: core and cladding radius are 2.625 μm and 62.5 μm. And at $\lambda = 1.55\mu$m, the refractive index of fiber core and cladding are 1.452 and 1.444, while that of the surrounding medium is 1.0 (Air).

Using the software, we determined the first 100 modes (including all degenerate states) with field profiles on a grid of 256×256 points in a range of ± 64 μm from fiber axis in both dimensions. The LP_{01} core mode has a much weaker dependence on the curvature of fiber because the diameter of fiber core is much smaller than that of fiber cladding. In order to observe the evolution of mode profiles clearly, we only selected several representative low-order cladding modes, whose intensity distributions are presented in Table I. The even $\mathrm{LP}^{\mathrm{e}}_{1\mathrm{m}}$ and odd $\mathrm{LP}^{\mathrm{o}}_{1\mathrm{m}}$ modes are defined as those are x-polarized and y-polarized and with lobes oriented above and below the $\mathrm{x} = 0$ and $\mathrm{y} = 0$ plane, respectively. According to the coupled mode theory, we should note that the coupling strength of cladding mode resonance is partially dependant on the field overlap integral in core region between core mode and cladding mode [17]. So the profiles at $C = 0$ indicate why the coupling strengths of $\mathrm{LP}_{0\mathrm{m}}$ cladding mode resonances is stronger than those of $\mathrm{LP}_{1\mathrm{m}}$ modes in a straight TFBG. We can see that $\mathrm{LP}_{0\mathrm{m}}$ modes have a local maximum intensity in the fiber core which results in a higher mode overlap with the LP_{01} core mode. But the $\mathrm{LP}_{1\mathrm{m}}$ modes have very low intensity in the fiber core, and thus the overlap with the core mode is also lower. As the fiber is bent (increasing curvature C), the intensity of LP_{02} and LP_{05} shift towards the outer portion of fiber. This shift introduces a decrease of the relative power residing within the fiber center

TABLE I
INTENSITY PROFILES OF SELECTED MODES AT DIFFERENT FIBER CURVATURES

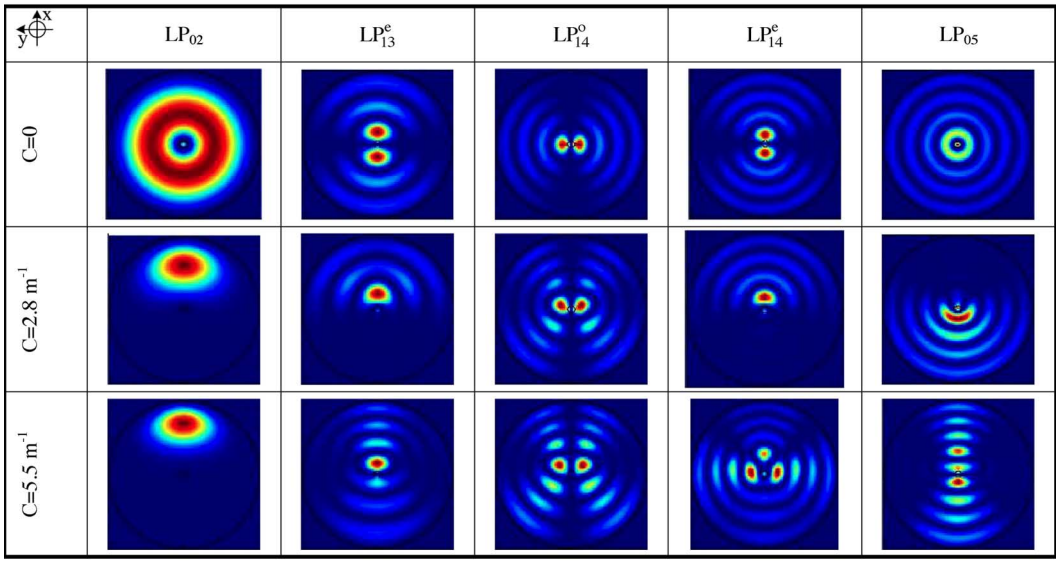

and consequently a reduction of overlap integral with the core mode. And as expected in the above-mentioned physical geometry of bent fiber, the intensity profile shift is accompanied with the changes in effective refractive index (LP_{05} mode: 1.4390 to 1.4388 at the curvature increasing from 0 m^{-1} to 5.5 m^{-1}), which will lead to a blue shift in the resonance wavelength of a bent TFBG. On the other hand, the LP^{o}_{1m} modes continue to have relatively low overlap with the core mode with increasing curvature. However, the LP^{e}_{1m} modes undergo more obvious variations (see Table I). The mode lobes shift along the x axis and bring some power in the fiber core region, which results in an increase of mode overlap with the core mode and thus strengthens the corresponding LP^{e}_{1m} cladding mode resonances in TFBG. We do not have quantitative calculation for the values of wavelength shift and resonance strength of TFBG because the effective tilted angle also varies with the bending curvature. But this study is quite a supportive explanation to the following experimental bending responses with R-TFBG. The differences among LP^{e}_{1m}, LP^{o}_{1m} and LP_{0m} cladding mode resonances provide a measure for determining the magnitude and direction of a bend simultaneously.

IV. BEND RESPONSE OF THE R-TFBG

The experimental investigation on the bend response of R-TFBG was carried out by using a similar setup with our previous work as reported in [17]. The R-TFBG was inserted into a polymer capillary and then bonded to a steel beam which laid on two movable supports and bent with a micrometer driver in the middle. The capillary can ensure the whole fiber adhere to the beam and avoid unwanted axial strain on the grating. The applied curvature of bending can be measured through the central displacement d of the R-TFBG by $C = 2d/(d^2 + L^2)$, where L is half of the distance of two supports. The ends of fiber were clamped by two rotatable fiber holders, which were employed to adjust the orientation of fiber and thus the direction of bend. The original direction is defined as 0° with respect to the tilted grating plane.

Fig. 3 shows the transmission spectra evolutions and amplitude changes of the selected resonances in R-TFBG against the applied curvature at the direction of 0°. As expected, the wavelength and amplitude of cladding mode resonances vary against the curvature. But here only the amplitude is of our interests and enough for determine both the direction and magnitude of bend. We can see the coupling strength of LP_{018} decreases but the even LP_{118} increases with the increasing applied curvature (see Fig. 3(a)). As the wavelength shift, the LP^{e}_{118} and LP^{o}_{118} cladding mode resonances overlapped with each other and only one resonance can be seen in the spectrum when the curvature reached to 8.1 m^{-1}. The LP_{018} mode split into two peaks by the bending induced birefringence in the bent fiber. The lower (13th) order cladding modes have similar responses at the beginning (see Fig. 3(b)), but it saturated soon as the curvature increased. Meanwhile, the Bragg mode resonance is very stable at all curvatures (see Fig. 3(c)) because the curvature rarely affects the field profile of core LP_{01} mode. The cladding mode and Bragg mode has a similar temperature sensitivity of 10 pm/°C, so the Bragg wavelength also can be used as an inherent thermometer for temperature compensation [19]. Fig. 3(d) shows the amplitude changes of the represented resonances. Among them, the 18th order cladding mode has the maximum curvature sensitivity but the higher order mode (23rd) has a better linear response. At a certain direction of bend, we may employ the differential amplitude change between LP_{0m} and LP_{1m} mode to eliminate the power fluctuation from the fiber line or light source and enhance the curvature sensitivity (0.4 dB. m for 18th order mode). The resolution of the curvature measurement is 0.025 m^{-1} if the relative power measurement accuracy is 0.01 dB. These properties make this system ideal for the measurement of large structures such as bridges, buildings and other built devices. Fig. 4(a) and (b) indicate the spectra evolutions of 18th order mode resonance in the R-TFBG at another two directions of 45° and 90°. If we focus on the responses of LP_{118} mode, we may find the amplitude of LP^{e}_{118} and LP^{o}_{118} cladding mode resonances decrease with similar curvature sensitivity for 45°.

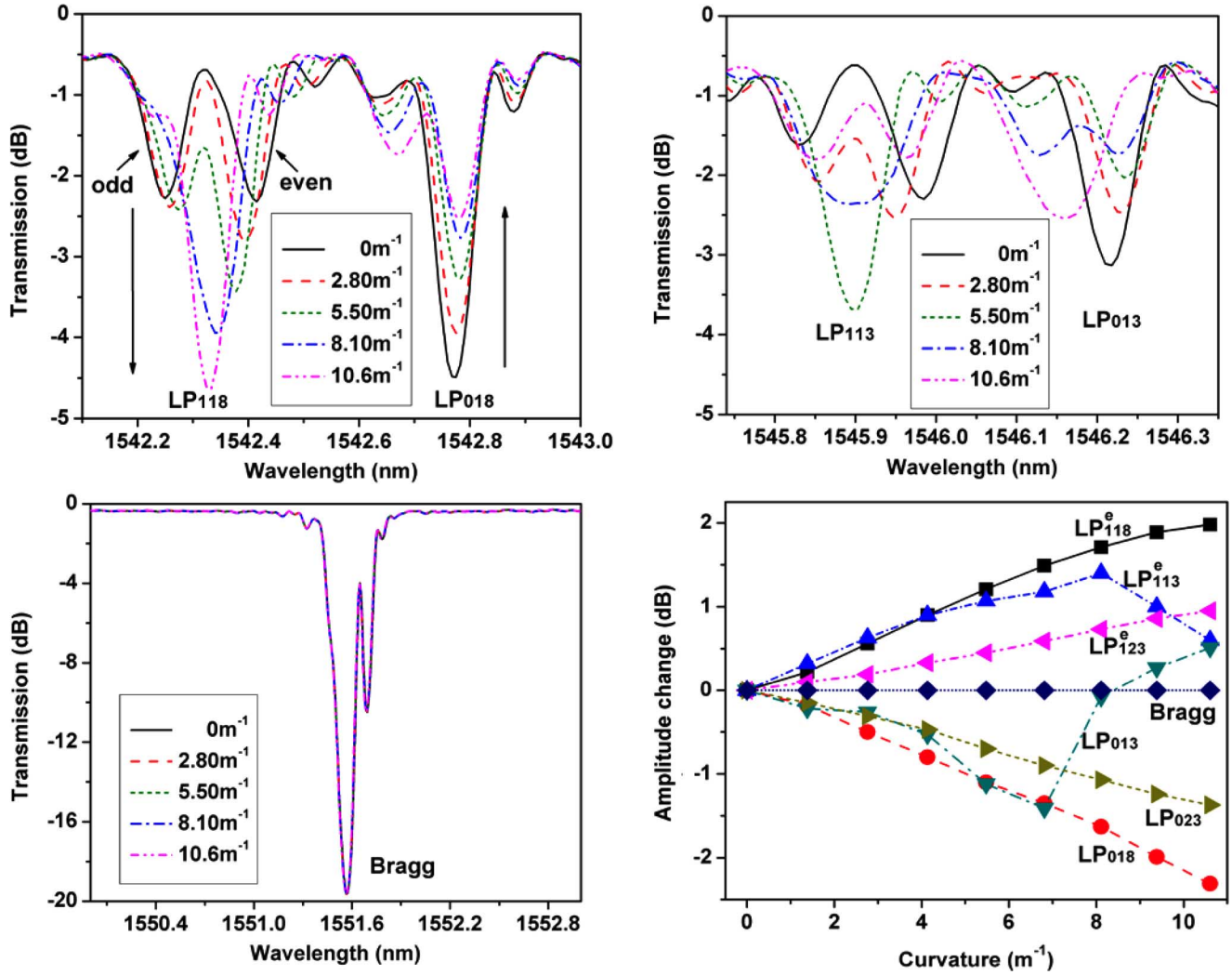

Fig. 3. Transmission spectra evolutions of R-TFBG at selected resonances against the applied curvature: (a) 18th and (b) 13th order cladding mode; (c) core Bragg mode. And (d) amplitude changes of the represented resonances against the applied curvature.

But the amplitude of $\mathrm{LP}^{\mathrm{o}}_{118}$ cladding mode has a higher sensitivity than that of $\mathrm{LP}^{\mathrm{e}}_{118}$ cladding mode at 90° (see Fig. 4(b)). Contrarily, the amplitude of $\mathrm{LP}^{\mathrm{e}}_{118}$ cladding mode decreases more drastically than that of $\mathrm{LP}^{\mathrm{o}}_{118}$ cladding mode at 0° (see Fig. 3(a)). By monitoring the amplitude difference changes between $\mathrm{LP}^{\mathrm{o}}_{118}$ and $\mathrm{LP}^{\mathrm{e}}_{118}$ cladding modes, we can determine the direction of the applied curvature. Fig. 4(c) demonstrates amplitude difference changes of odd and even LP_{118} modes ($\mathrm{A_o}$ and $\mathrm{A_e}$ are the amplitudes of $\mathrm{LP}^{\mathrm{o}}_{118}$ and $\mathrm{LP}^{\mathrm{e}}_{118}$ mode resonances, respectively). Noting that the two modes overlapped as the applied curvature increases up to 8.1 m^{-1}, the measurable curvature range with recognition of direction is limited by this effect. The dynamic range is not so high but is sufficient for most applications such as the structural health monitoring of bridges, buildings or other large structures (the TFBG sensor can also be attached to another mechanical actuator to increase the dynamic range if needed). As the direction of the bend is determined, the differential amplitude change between LP_{118} and LP_{018} cladding mode resonances can be calibrated. Thus, the direction and magnitude of a bend are measured by monitoring the amplitudes of a selected set of neighboring LP_{118} and LP_{018} cladding mode. We may add that there are also small resonance wavelength changes associated with bending (Figs. 3(a), 4(a), and (b)), of the order of a few tens of pm, but it is our experience that it is easier to measure amplitude changes (especially relative amplitude changes) than wavelength ones for changes of this magnitude. Furthermore the relative amplitude measurements are independent of the absolute power levels in the fiber. Finally, if interrogation cost is an issue, the relative amplitude measurement can be carried out with two band pass filters and photodetectors instead of an Optical Spectrum Analyzer.

V. Conclusion

We have written a re-grown TFBG in a small-core single mode fiber (Corning Flexcore) with UV overexposure. The fabricated R-TFBG shows a unique spectrum compared to those of normal TFBG (Type I) in SMF-28 fiber. There is a large difference in the amplitude between neighboring symmetric $(\mathrm{LP}_{0\mathrm{m}})$ and asymmetric $(\mathrm{LP}_{1\mathrm{m}})$ cladding mode resonances and each asymmetric cladding mode resonance splits into two peaks (related to two orthogonal polarization states). The amplitudes of symmetric and asymmetric cladding mode resonances change in

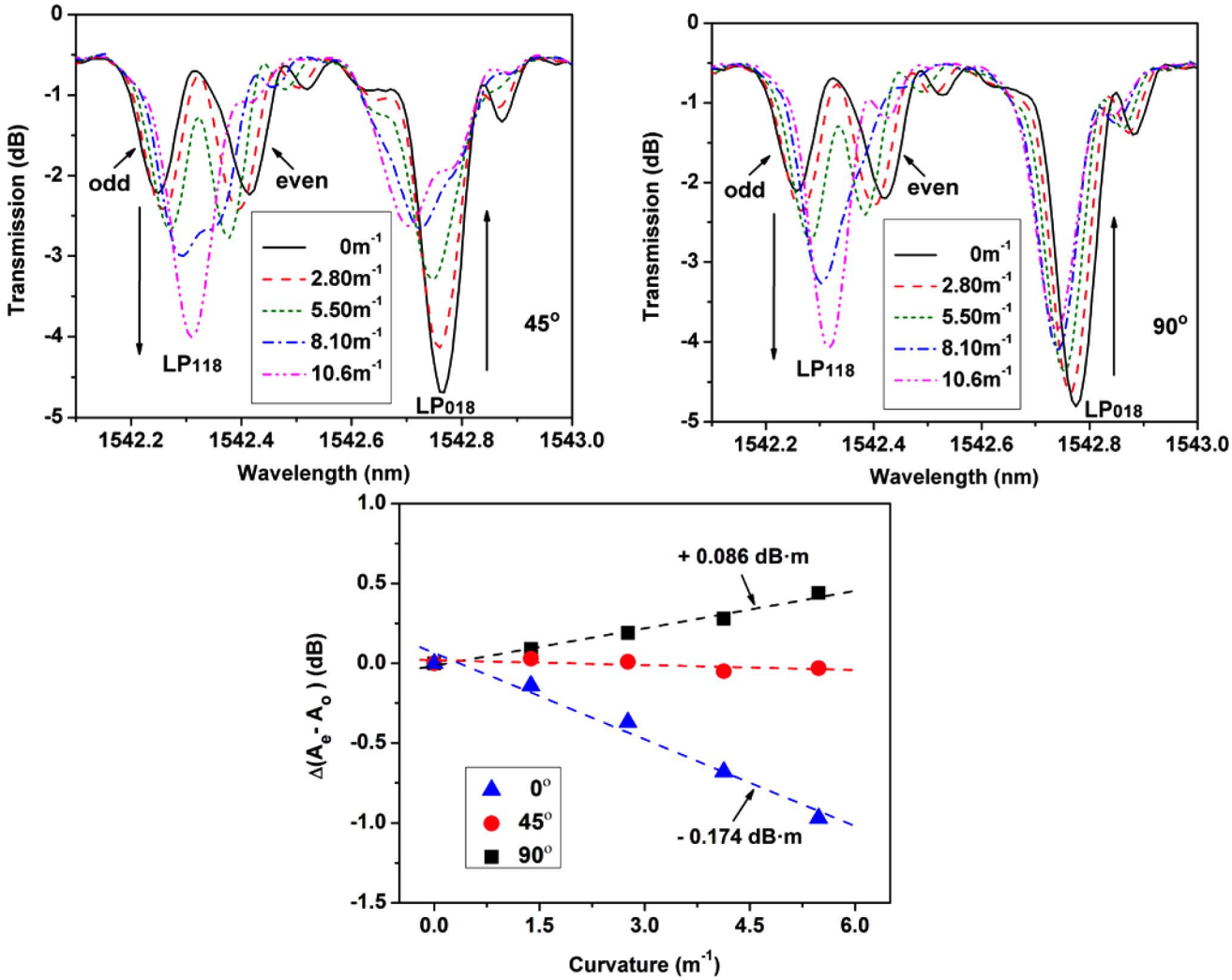

Fig. 4. Transmission spectra evolutions of 18th order mode resonance in the R-TFBG at another two directions of (a) 45° and (b) 90° against the applied curvature. And (c) the amplitude difference changes of odd and even LP_{118} modes (A_o and A_e are the amplitudes of LP^{o}_{118} and LP^{e}_{118} mode resonances, respectively).

opposite direction if the TFBG is bent. Numerical simulations show that the directional bend response is partially caused by the changes of coupling strength from fundamental core mode to both symmetric and asymmetric cladding modes. Experimental results prove that the magnitude and direction can be determined simultaneously by monitoring the amplitude difference changes among three selected neighboring resonances of the same order For this purpose the 18th order cladding mode resonance of the R-TFBG in the Flexcore fiber is the most suitable because it has the maximum curvature sensitivity and its lower linearity can be compensated by nonlinear calibration of its response. The proposed device is simple and easy to fabricate so that it has a promising perspective in practical application for shape sensing or vector bending measurement.

ACKNOWLEDGMENT

The authors will also thank Lumerical Solutions for providing a trial version of Mode Solutions 4.0.

REFERENCES

[1] Y. J. Rao, "In-fibre Bragg grating sensors," *Meas. Sci. Technol.*, vol. 8, no. 4, pp. 355–375, Apr. 1997.

[2] H.-J. Sheng, W.-F. Liu, K.-R. Lin, S.-S. Bor, and M.-Y. Fu, "High-sensitivity temperature-independent differential pressure sensor using fiber Bragg gratings," *Opt. Exp.*, vol. 16, no. 20, pp. 16013–16018, Sep. 2008.

[3] L. Jin, Z. Wang, Q. Fang, Y. G. Liu, B. Liu, G. Y. Kai, and X. Y. Dong, "Spectral characteristics and bend response of Bragg gratings inscribed in all-solid bandgap fibers," *Opt. Exp.*, vol. 15, no. 23, pp. 15555–15565, Nov. 2007.

[4] D. H. Zhao, X. F. Chen, K. M. Zhou, L. Zhang, I. Bennion, W. N. MacPherson, J. S. Barton, and J. D. C. Jones, "Bend sensors with direction recognition based on long-period gratings written in D-shaped fiber," *Appl. Opt.*, vol. 43, no. 29, pp. 5425–5428, Oct. 2004.

[5] T. Allsop, M. Dubov, A. Martinez, F. Floreani, I. Khrushchev, D. J. Webb, and I. Bennion, "Bending characteristics of fiber long-period gratings with cladding index modified by femtosecond laser," *J. Lightw. Technol.*, vol. 24, no. 8, pp. 3147–3154, Aug. 2006.

[6] Z. H. He, Y. N. Zhu, and H. Du, "Effect of macro-bending on resonant wavelength and intensity of long-period gratings in photonic crystal fiber," *Opt. Exp.*, vol. 15, no. 4, pp. 1804–1810, Feb. 2007.

[7] G. M. H. Flockhart, W. N. MacPherson, J. S. Barton, J. D. C. Jones, L. Zhang, and I. Bennion, "Two axis bend measurement with Bragg gratings in multicore optical fiber," *Opt. Lett.*, vol. 28, no. 6, pp. 387–389, Mar. 2003.

[8] K. H. Smith, B. L. Ipson, T. L. Lowder, A. R. Hawkins, R. H. Selfridge, and S. M. Schultz, "Surface-relief fiber Bragg gratings for sensing applications," *Appl. Opt.*, vol. 45, no. 8, pp. 1669–1675, Mar. 2006.
[9] S. Baek, Y. Jeong, and B. Lee, "Characteristics of short-period blazed fiber Bragg gratings for use as macro-bending sensors," *Appl. Opt.*, vol. 41, no. 4, pp. 631–636, Feb. 2002.
[10] T. Guo, L. Y. Shao, H.-Y. Tam, P. A. Krug, and J. Albert, "Tilted fiber grating accelerometer incorporating an abrupt biconical taper for cladding to core recoupling," *Opt. Exp.*, vol. 17, no. 23, pp. 20651–20660, Oct. 2009.
[11] L. Y. Shao and J. Albert, "Compact fiber-optic vector inclinometer," *Opt. Lett.*, vol. 35, no. 7, pp. 1034–1036, Mar. 2010.
[12] K. S. Lee and T. Erdogan, "Fiber mode coupling in transmissive and reflective tilted fiber gratings," *Appl. Opt.*, vol. 39, no. 9, pp. 1394–1404, Mar. 2000.
[13] A. G. Simpson, K. Kalli, K. Zhou, L. Zhang, and I. Bennion, "Formation of type IA fibre Bragg gratings in germanosilicate optical fibre," *Electron. Lett.*, vol. 40, no. 3, pp. 163–164, Feb. 2004.
[14] D. Marcuse, "Field deformation and loss caused by curvature of optical fibers," *J. Opt. Soc. Amer.*, vol. 66, no. 4, pp. 311–320, Apr. 1976.
[15] U. L. Block, M. J. F. Digonnet, M. M. Fejer, and V. Dangui, "Bending-induced birefringence of optical fiber cladding modes," *J. Lightw. Technol.*, vol. 24, no. 6, pp. 2336–2339, Jun. 2006.
[16] [Online]. Available: http://www.lumerical.com/mode_solver_description.php#mode_overview
[17] T. Erdogan and J. E. Sipe, "Tilted fiber phase gratings," *J. Opt. Soc. Amer. A*, vol. 13, no. 2, pp. 296–313, Feb. 1996.
[18] L. Y. Shao, A. Laronche, M. Smietana, P. Mikulic, W. J. Bock, and J. Albert, "Highly sensitive bend sensor with hybrid long-period and tilted fiber Bragg grating," *Opt. Commun.*, vol. 283, no. 13, pp. 2690–2694, Jul. 2010.
[19] L. Y. Shao, Y. Shevchenko, and J. Albert, "Intrinsic temperature sensitivity of tilted fiber Bragg grating based surface plasmon resonance sensors," *Opt. Exp.*, vol. 18, no. 11, pp. 11464–11471, May 2010.

Li-Yang Shao received the B.Sc. degree in 2001 and the Ph.D. in 2008 in optical engineering, both from Zhejiang University, China.

From 2001 to 2002 he was with O-NET Communications Ltd. in China, as a research engineer working on passive optical components for DWDM system. From 2006 to 2009, he was with The Hong Kong Polytechnic University, first as a Research Assistant, then as a Research Associate working on fiber grating devices and sensors. Currently, he is a Post Doctoral Fellow at the Department of Electronics at Carleton University in Canada. His current research interests are fiber gratings, fiber lasers and sensors, fiber-optic SPR sensors. He has authored/coauthored over 30 papers in the refereed international journals/conferences. He has also been the Technical Program Committee of the International Conference on Advance Infocomm Technology (ICAIT) since 2008.

Lingyun Xiong received the B.Sc. degree in 2001 and the M.Sc. degree in 2004 in Optics from Nankai University, China, as well as the M.A.Sc. degree in electronics engineering from Carleton University, Canada, in 2007, where he is currently working toward the Ph.D. degree in Department of Electronics.

His research interests include Bragg gratings in advanced doping glass fibers, and their application in fiber lasers.

Chengkun Chen, photograph and biography not available at time of publication.

Albane Laronche, photograph and biography not available at time of publication.

Jacques Albert received the degrees in physics from Université de Montréal (1978) and Laval University (1980), and the Ph.D. degree in electrical engineering from McGill University, Canada, in 1988.

He has held the Canada Research Chair in Advanced Photonics Components at Carleton University since 2004. Prior to his appointment at Carleton, he had R&D positions with Alcatel Optronics Canada and with the Communications Research Center of Canada. He is coauthor of over 180 publications in journals and conference proceedings and is co-inventor on three patents (and several patent applications). He has been on the Technical Committee of the Optical Society of America Topical Meeting on Bragg Gratings, Photosensitivity and Poling since 1997 and was General Co-chair of the last two meetings in Sydney (Australia), in 2005 and Quebec City in 2007.

Dr. Albert is currently Associate Editor of *Optics Express* and co-chair of the upcoming Symposium on novel optical fibers at the 2010 Conference on Lasers and Electro-Optics (CLEO) as well as Program co-Chair of Optical Fiber Sensors (OFS-21) for 2011.